



## Short communication

# Synthesis and reversible lithium storage of $\text{Cr}_2\text{O}_5$ as a new high energy density cathode material for rechargeable lithium batteries

Xu-Yong Feng, Ning Ding, Li Wang, Xiao-Hang Ma, Yong-Ming Li, Chun-Hua Chen\*

CAS Key Laboratory of Materials for Energy Conversions, Department of Materials Science and Engineering, University of Science and Technology of China, Anhui Hefei 230026, China

## H I G H L I G H T S

- Pure  $\text{Cr}_2\text{O}_5$  is prepared by the thermal decomposition of  $\text{CrO}_3$  under ambient atmosphere at 350–400 °C.
- Reversible lithiation/de-lithiation of  $\text{Cr}_2\text{O}_5$  proceeds via a single phase process.
- $\text{Cr}_2\text{O}_5$  electrode can reach a high energy density of 819 Wh  $\text{kg}^{-1}$  with good cyclability and high energy efficiency (83%).

## A R T I C L E I N F O

## Article history:

Received 18 April 2012

Received in revised form

2 August 2012

Accepted 22 August 2012

Available online 28 August 2012

## Keywords:

Chromium oxide

Ex-situ X-ray diffraction

Energy density

Cyclic voltammogram

Lithium batteries

## A B S T R A C T

Chromium trioxide is calcined from 350 to 400 °C yielding pure  $\text{Cr}_2\text{O}_5$ . The electrochemical properties of the resulting chromium oxides have been measured in the potential range 2.0–4.5 V (vs.  $\text{Li}^+/\text{Li}$ ) when used in lithium batteries. The first discharge process, the intercalation of lithium into  $\text{Cr}_2\text{O}_5$ , proceeds via two steps. In the following cycles, lithium is found to be reversibly de-lithiated/lithiated via a solid solution process with an un-known single phase  $\text{Li}_x\text{Cr}_2\text{O}_5$  (*u*-phase) characterized by an X-ray diffractive lattice spacing of about 0.20 nm. The sample that results from chromium trioxide being calcined at 350 °C shows the highest capacity of 273 mAh  $\text{g}^{-1}$  (the first discharge at 0.5 C rate) and the sample calcined at 400 °C shows the best cyclability with the capacity retention of 96% after 100 cycles. The energy density of  $\text{Cr}_2\text{O}_5$  can reach 819 Wh  $\text{kg}^{-1}$  with the energy conversion efficiency of 83%.

© 2012 Elsevier B.V. All rights reserved.

## 1. Introduction

Transition metal oxides have attracted increasing interests as electrode materials of rechargeable lithium batteries for their high specific capacities of usually over 500 mAh  $\text{g}^{-1}$  compared with the theoretical 372 mAh  $\text{g}^{-1}$  of the state-of-the-art graphite. Most of these oxides, such as NiO [1–3], CoO [4–6] and CuO [7–9], can only be used as anodes due to their low working potentials (around 1.0 V vs. Li). However, high valence transition metal oxides, such as  $\text{VO}_x$  ( $\text{VO}_2$  [10,11],  $\text{V}_2\text{O}_5$  [12,13]) and  $\text{MoO}_3$  [14], can react with lithium at a potential over 2.0 V vs. Li, and thus can be potentially used as cathode materials. Different from the situation of NiO or CoO, where lithiation process proceeds via a conversion reaction

mechanism [15], lithium can reversibly intercalate into and de-intercalate from  $\text{VO}_x$  and  $\text{MoO}_3$  during the charge and discharge processes. Their initial capacity loss is much lower and energy efficiency is much higher than those of CoO, NiO and CuO, due to the different lithium storage mechanism. Some high valence chromium oxides such as  $\text{Cr}_8\text{O}_{21}$ ,  $\text{Cr}_3\text{O}_8$  and  $\text{CrO}_2$  can also store Li via intercalation reaction mechanism, and thus are promising cathode materials for their high specific capacities of over 200 mAh  $\text{g}^{-1}$  [16–21]. Another interesting high valence chromium oxide for reversible lithium intercalation is  $\text{Cr}_2\text{O}_5$  [22–24], which is found as the main component of so-called “Seloxcette” or the product of  $\text{CrO}_3$  intercalation in graphite [24]. However, the synthesis of the high valence chromium oxides usually carried out in an autoclave under high oxygen pressure, which is relatively difficult and dangerous. Also, without appropriately defining the potential range, the electrochemical cyclability of these chromium oxides is relatively poor. In this work, we calcine  $\text{CrO}_3$  to synthesize  $\text{Cr}_2\text{O}_5$  in only ambient conditions at the temperatures from 350 °C to 400 °C. It operates via a not reported solid solution process in the

\* Corresponding author. Tel.: +86 551 3606971; fax: +86 551 3601952.  
E-mail address: [cchchen@ustc.edu.cn](mailto:cchchen@ustc.edu.cn) (C.-H. Chen).

potential range 2.0–4.5 V (vs.  $\text{Li}^+/\text{Li}$ ) and gives good performance with an energy density as high as  $819 \text{ Wh kg}^{-1}$ .

## 2. Experimental

Chromium oxides were synthesized via the thermal decompositions of a commercial  $\text{CrO}_3$  powder (Sinopharm Chemical Reagent Co., Ltd) at various temperatures from  $300^\circ\text{C}$  to  $425^\circ\text{C}$  in air for 2 h. After the heat treatment, the products were ground in an agate mortar into fine powders. Thermogravimetric analysis (TGA) was applied to investigate the decomposition process of  $\text{CrO}_3$  at the heating rate of  $3^\circ\text{C min}^{-1}$  in air. The crystal structures of the decomposition products were characterized by X-ray diffraction (XRD,  $\text{CuK}\alpha$  radiation, DX-2700).

The electrochemical performance of the obtained samples was measured in the CR2032 coin-type half cells with 1 M  $\text{LiPF}_6$  in EC:DMC (1:1 v/v) as the electrolyte. The electrodes consisted of a mixture of 80 wt% chromium oxides, 10 wt% carbon black and 10 wt% PVDF binder on Al foil. The cells were assembled in an argon-filled dry-box (MBraun Labmaster 130) and cycled on a multi-channel battery test system (NEWARE BTS-610) at the constant current in the voltage range from 2.0 to 4.5 V. Cyclic voltammograms (CV) of the cells were also measured on a CHI 660 Electrochemical Workstation in the voltage range from 2.0 to 4.5 V at the scanning rate of  $0.1 \text{ mV s}^{-1}$ .

To investigate the lithium intercalation process into  $\text{Cr}_2\text{O}_5$ , an ex-situ XRD analysis was carried out on the sample obtained at  $350^\circ\text{C}$ . The cells were cycled at C/16 (0.1 mA) and were disassembled at different charge–discharge states. The lithiated electrodes were washed by dimethyl carbonate (DMC) to remove the electrolyte residue. After drying in the argon-filled glove box, the XRD analyses of these electrodes were immediately performed in dry air with a scan rate of  $1^\circ \text{ min}^{-1}$ .

## 3. Results and discussion

TGA curve (Fig. 1a) shows the thermal decomposition process of  $\text{CrO}_3$ .  $\text{CrO}_3$  starts to decompose at around  $250^\circ\text{C}$  and ends at  $475^\circ\text{C}$ . The step-like TG curve indicates that the decomposition of  $\text{CrO}_3$  can be roughly divided into two stages: (1) from 250 to  $400^\circ\text{C}$ , the weight loss is 18%; (2) from 400 to  $475^\circ\text{C}$ , the corresponding weight loss is 13%. According to the XRD patterns (Fig. 1b),  $\text{Cr}_8\text{O}_{21}$  and  $\text{Cr}_2\text{O}_5$  are formed at  $300^\circ\text{C}$ . Pure  $\text{Cr}_2\text{O}_5$  is obtained in the temperature range from  $350$  to  $400^\circ\text{C}$  but it further decomposes into  $\text{Cr}_2\text{O}_3$  at  $425^\circ\text{C}$ . Obviously, the weight loss in the first TG stage (18%) is markedly higher than the value (8%) predicted based on the conversion from  $\text{CrO}_3$  to  $\text{Cr}_2\text{O}_5$ . This is due to the volatilization of  $\text{CrO}_3$  at temperatures above its melting point  $196^\circ\text{C}$ , as also observed by Liu et al. [18]. On the other hand, the weight loss in the second stage matches very well with the theoretical value because  $M(\text{Cr}_2\text{O}_5)/M(\text{Cr}_2\text{O}_3) = 1.21 \approx 82\%/69\%$ , meaning that the results of TGA and XRD agree with each other. As an example of the decomposition products from  $\text{CrO}_3$ , the morphology of  $\text{Cr}_2\text{O}_5$  sample obtained at  $375^\circ\text{C}$  (Fig. 1a) shows that the powder is composed of flaky particles.

Because the samples calcined at  $350^\circ\text{C}$  to  $400^\circ\text{C}$  are  $\text{Cr}_2\text{O}_5$ , which has not been investigated as a cathode material for lithium batteries, they are then focused in this work. Their first discharge and charge profiles (Fig. 2a) indicate that the first discharge process can be divided into two parts: (1) a short voltage slope from 3.2 to 2.9 V; (2) a long voltage plateau at about 2.9 V. The short slope should be related to a solid solution process and the plateau should be related to a two-phase reaction. It is noticed that the first discharge capacity decreases with increasing the calcination temperature. All of these  $\text{Cr}_2\text{O}_5$  samples exhibit good cycling

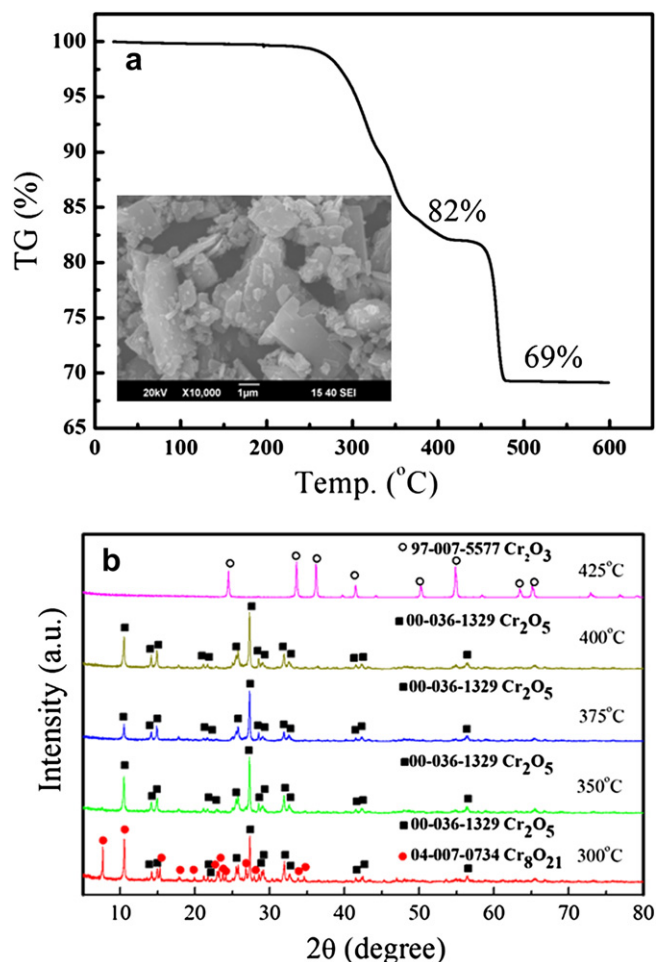
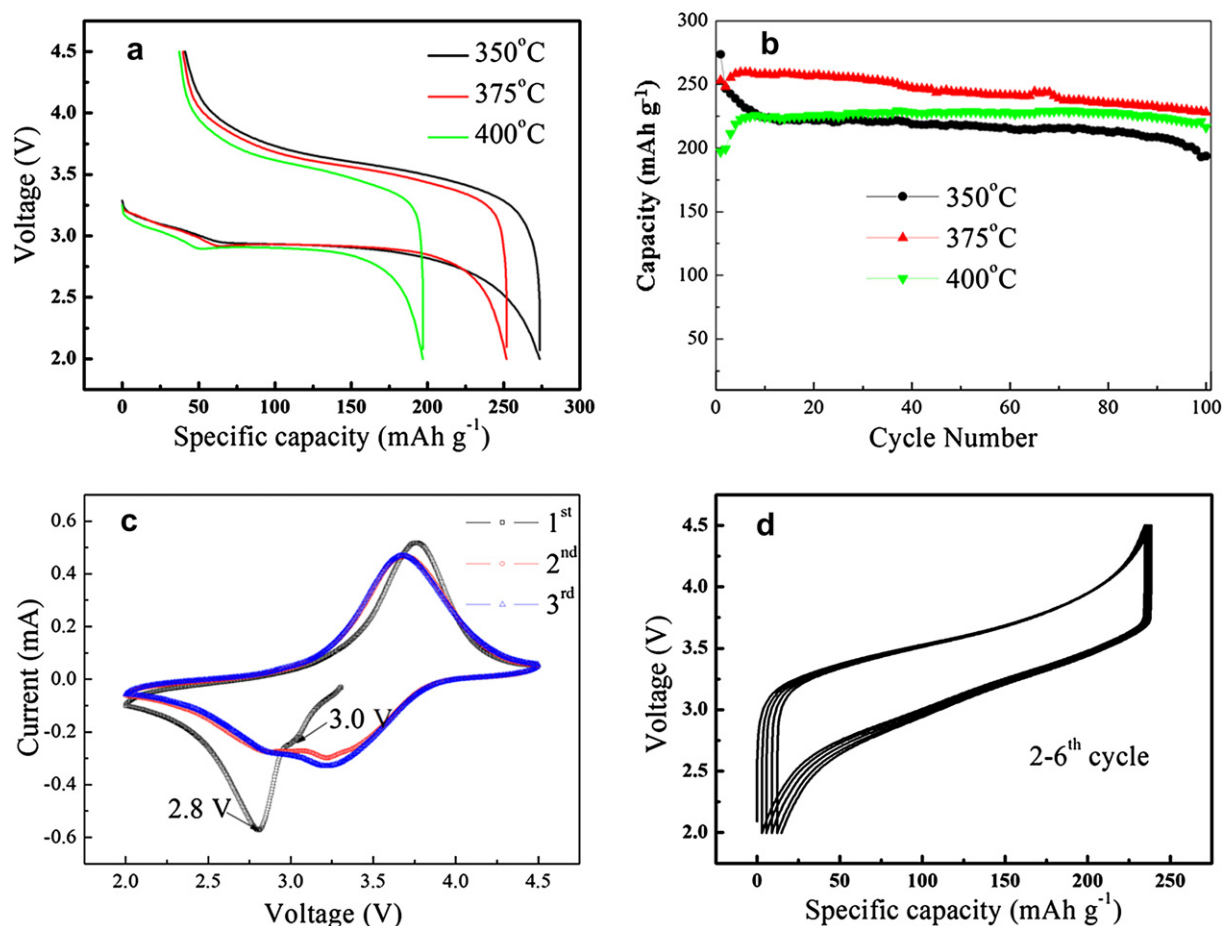


Fig. 1. TG curve (a) of  $\text{CrO}_3$  and XRD patterns (b) of calcined samples.

performance (Fig. 2b). Particularly, the  $400^\circ\text{C}$ -calcined sample delivers a high capacity of  $220 \text{ mAh g}^{-1}$  with the best cycling performance.

To investigate the lithium intercalation process into  $\text{Cr}_2\text{O}_5$ , an ex-situ XRD analysis was carried out on the sample calcined at  $350^\circ\text{C}$  (Fig. 3). From state A to B in the first discharge process, the peak at about  $27^\circ$  (marked with #) becomes weaker and the peaks at  $28^\circ$  and  $30^\circ$  grow wider and combine together. Nevertheless, there is a very minor change when discharged from A to B. From the state B to F, a new peak at around  $45^\circ$  (marked with \*) is detected and its intensity increases with lithium intercalation, while other peaks become weaker and weaker until they disappear. This phenomenon implies that during the states from B to F,  $\text{Cr}_2\text{O}_5$  reacts with lithium to form an un-identified phase (*u*-phase  $\text{Li}_x\text{Cr}_2\text{O}_5$ ) with a characteristic diffraction peak at around  $45^\circ$ . According to Bragg's law, this diffraction angle ( $2\theta = 45^\circ$ ) corresponds to a lattice spacing of about 0.20 nm. Based on the voltage profile (Fig. 3a), the lithiated sample at 2.0 V (state F) should be  $\text{Li}_{2.2}\text{Cr}_2\text{O}_5$ .

In the following charge process (from state F to K in Fig. 3), the diffraction peak at around  $45^\circ$  remains but shifts by  $0.2^\circ$  to the higher angle direction, suggesting that the de-lithiation is via a solid solution process of the *u*- $\text{Li}_x\text{Cr}_2\text{O}_5$ . The ex-situ XRD results are further confirmed by the CV curve (Fig. 2c). In the first cycle, there are two reduction peaks at 3.0 V and 2.8 V, and only one oxidation peak at 3.7 V. In the following cycles, the CV curves are almost overlapped, indicating that the lithiation/de-lithiation processes are highly reversible (Fig. 2d). After full charge, the



**Fig. 2.** Electrochemical performance of synthesized  $\text{Cr}_2\text{O}_5$ : (a) the first discharge and charge profiles, (b) cycling performance, (c) cyclic voltammograms of the 350 °C-calcined sample, and (d) voltage profiles of the 350 °C-calcined sample.

XRD pattern does not go back to the initial state, which means that the first electrochemical reduction process of  $\text{Cr}_2\text{O}_5$  by lithium form the reversible  $u\text{-Li}_x\text{Cr}_2\text{O}_5$  of a different crystal structure. The average working potential of  $u\text{-Li}_x\text{Cr}_2\text{O}_5$  is about 3.17 V, which results in a maximum energy density of  $819 \text{ Wh kg}^{-1}$  for the 375 °C sample. Besides, the energy conversion efficiency of  $\text{Cr}_2\text{O}_5$  is about

83%, which is much higher than other transition metal oxides, such as  $\text{CoO}$  (54.6%) [15] and  $\text{RuO}_2$  (54.9%) [25]. On the other hand, as indicated in Fig. 2d, the rather large voltage difference, about 0.5 V, in the charging and discharging potential suggests that the rate capability of current sample is not optimal and needs further improvement.

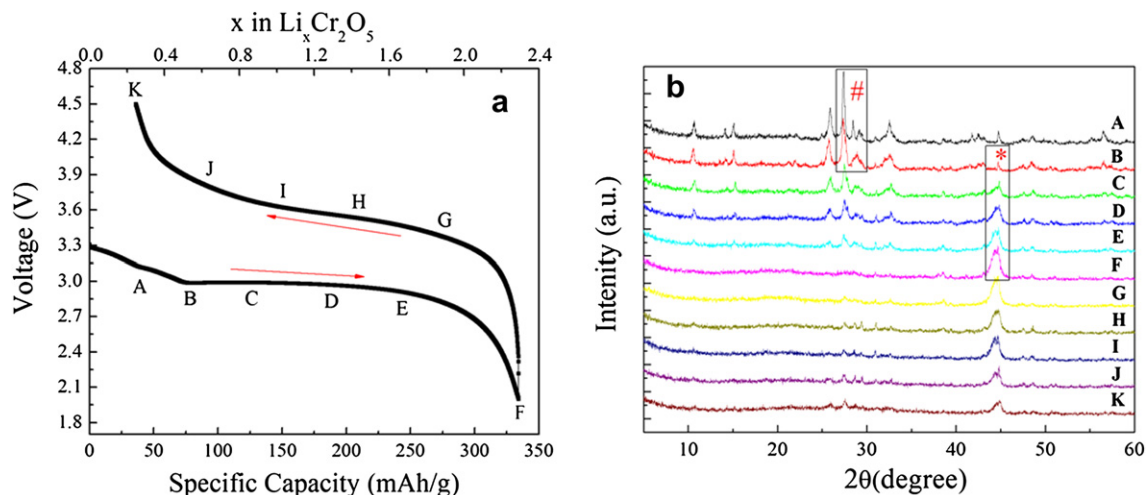


**Fig. 3.** Ex-situ XRD of the 350 °C sample cycled between 2.0 V and 4.5 V.

#### 4. Conclusions

Pure  $\text{Cr}_2\text{O}_5$  can be prepared via thermal decomposition of  $\text{CrO}_3$  in ambient pressure between 350 °C and 400 °C. The sample calcined at 350 °C shows the highest capacity of  $273 \text{ mAh g}^{-1}$  and the sample calcined at 400 °C shows the most excellent cyclability with the capacity retention of 96% after 100 cycles. Considering the high energy density and high energy conversion efficiency,  $\text{Cr}_2\text{O}_5$  can be potentially used in the high energy lithium batteries.

#### Acknowledgments

This study was supported by National Science Foundation of China (grant nos. 20971117 and 10979049) and Education Department of Anhui Province (grant no. KJ2009A142). We are also grateful to the Solar Energy Operation Plan of Academia Sinica.

#### References

- [1] X.F. Li, A. Dhanabalan, C.L. Wang, J. Power Sources 196 (2011) 9625.
- [2] Y.J. Mai, J.P. Tu, X.H. Xia, C.D. Gu, X.L. Wang, J. Power Sources 196 (2011) 6388.
- [3] J. Zhong, X.L. Wang, X.H. Xia, C.D. Gu, J.Y. Xiang, J. Zhang, J.P. Tu, J. Alloys Compd 509 (2011) 3889.
- [4] K.M. Nam, Y.C. Choi, S.C. Jung, Y. Kim, M.R. Jo, S.H. Park, Y.M. Kang, Y.K. Han, J.T. Park, Nanoscale 4 (2012) 473.
- [5] J.X. Zhu, Y.K. Sharma, Z.Y. Zeng, X.J. Zhang, M. Srinivasan, S. Mhaisalkar, H. Zhang, H.H. Hng, Q.Y. Yan, J. Phys. Chem. C 115 (2011) 8400.
- [6] L.J. Zhang, P. Hu, X.Y. Zhao, R.L. Tian, R.Q. Zou, D.G. Xia, J. Mater. Chem. 21 (2011) 18279.
- [7] J.S. Zhou, L.L. Ma, H.H. Song, B. Wu, X.H. Chen, Electrochem. Commun. 13 (2011) 1357.
- [8] X.H. Huang, C.B. Wang, S.Y. Zhang, F. Zhou, Electrochim. Acta 56 (2011) 6752.
- [9] Z.Y. Wang, F.B. Su, S. Madhavi, X.W. Lou, Nanoscale 3 (2011) 1618.
- [10] C.Z. Wu, Z.P. Hu, W. Wang, M. Zhang, J.L. Yang, Y. Xie, Chem. Commun. 33 (2008) 3891.
- [11] N. Ding, X.Y. Feng, S.H. Liu, J. Xu, X. Fang, I. Lieberwirth, C.H. Chen, Electrochem. Commun. 11 (2009) 538.
- [12] M. Sathiya, A.S. Prakash, K. Ramesha, J.-M. Tarascon, A.K. Shukla, J. Am. Chem. Soc. 133 (2011) 16291.
- [13] N.A. Galiote, M.N.L. Camargo, R.M. Iost, F. Crespilho, F. Huguenin, Langmuir 27 (2011) 12209.
- [14] K. Dewangan, N.N. Sinha, P.K. Sharma, A.C. Pandey, N. Munichandraiah, N.S. Gajbhiye, CrystEngComm 13 (2011) 927.
- [15] P. Poizot, S. Laruelle, S. Grugeon, L. Dupont, J.M. Tarascon, Nature 407 (2000) 496.
- [16] R.P. Ramasamy, P. Ramadass, B.S. Haran, B.N. Popov, J. Power Sources 124 (2003) 155.
- [17] P. Norby, A.N. Christensen, H. Fjellvag, M. Nielsen, J. Solid State Chem. 94 (281) (1991).
- [18] J.Y. Liu, Z.X. Wang, H. Li, X.J. Huang, Solid State Ionics 177 (2006) 2675.
- [19] P. Arora, D. Zhang, B.N. Popov, R.E. White, Electrochem. Solid-State Lett. 1 (1998) 249.
- [20] R.P. Ramasamy, B. Veeraraghavan, B. Haran, B.N. Popov, J. Power Sources 124 (2003) 197.
- [21] V. Sivakumar, C.A. Ross, N. Yabuuchi, Y. Shao-Horn, K. Persson, G. Ceder, J. Electrochem. Soc. 155 (2008) 83.
- [22] M.B. Armand, in: W. van Gool (Ed.), Fast Ion Transport in Solids, North-Holland, Amsterdam, 1973, p. 665.
- [23] M.S. Whittingham, Prog. Solid State Chem. 12 (1978) 41.
- [24] J.O. Besenhard, R. Schollhorn, J. Electrochem. Soc. 124 (1977) 968.
- [25] P. Balaya, H. Li, L. Kienle, J. Maier, Adv. Funct. Mater. 13 (2003) 621.